Contents

1 Perturbation of the spin motion

Blah-blah about the "Spin field" of the spin precession axes of beam particles.

Consequently, it is a source of systematic error for the FD method, in which we observe the polarization vector's precession frequency, since it varies during measurement due to this effect. Two points:

- the variation is stable; i.e., the variation occurs about a constant value, and there's no frequency creep.
- the frequency variation translates into a polarization measurement error, but that error is small compared to other polarimetry errors, and since it doesn't introduce a growth trend, it can be neglected.

Due to these reasons, we will neglect this effect in further considerations, assuming that all beam particles' spins precess about the closed orbit spin precession axis.

1.1 Simulation

We analized the effects of the spin precession axis motion on measurement data. In order to do so, we tracked an ensemble of particles offset from the reference orbit in the x and y cooridnates (but not in $\delta = \Delta p/p_0$), i.e. doing betatron oscillations alone. We collected the following data:

- spin tune $\nu_s(Z)$ and the spin precession axis components $n_x(Z)$, $n_y(Z)$, $n_z(Z)$, where $Z = (x, a, y, b, t, d)$ is the particle coordinate in phase space. [1, p. 9]
- the spin coordinates S_x, S_y, S_z,

The simulation was done with an FS lattice, at 270.0092 MeV, with an added spin kick 10^{-2} about the radial axis. The value for the kick was picked so as to reduce tracking time.

2 Spin decoherence in a perfectly aligned ring

Spin coherence refers to a measure or quality of preservation of polarization in an initially fully polarized beam. [1, p. 205]

When a polarized beam is injected into a storage ring, the spins of the beam particles start precessing around the vertical (guiding) magnetic field. The precession frequency is dependent upon the equilibrium-level energy of the particle, which differs for the particles in the beam.

This does not pose a problem when the initial polarization is vertical; however, the FS storage ring method requires spin polarization along the momentum vector, i.e., in the horizontal plane. Therefore, spin decoherence is an inherent weakness of the FS method.

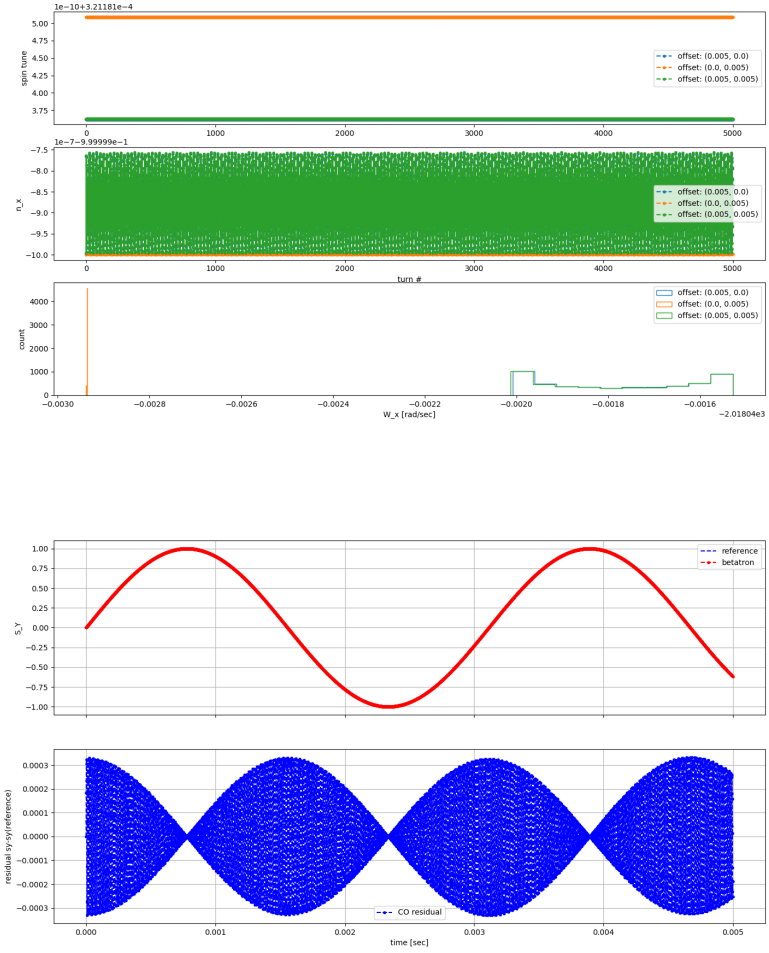

2.1 Spin coherence time requirements

The spin coherence time (SCT) for an FS method performed in a perfectly aligned storage ring is determined by the smallest detectable angle by which the beam polarization vector is tilted from the horizontal plane by EDM alone. For the sensitivity level of 10^{-29} $e \cdot cm$ it is about $5 \cdot 10^{-6}$. [2]

According to the T-BMT equation,

$$\Omega_{EDM,x} = \eta \frac{qE_x}{2mc},$$

where η is the proportionality factor between the EDM and spin, equaling 10^{-15} for the deuteron, for the given EDM sensitivity limit. [1, p. 206]

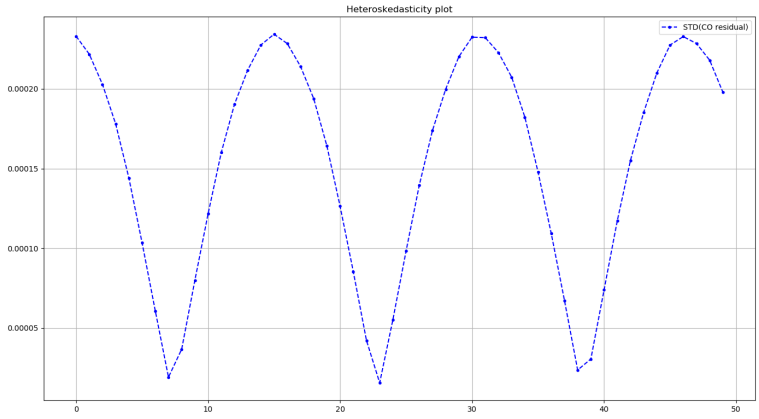

For the deuteron BNL FS storage ring, $E_x = 12$ MV/m, [2, p. 19] and so $\Omega_{EDM,x} \approx 10^{-9}$ rad/sec. This gives an SCT of approximately 1000 seconds in order that the vertical polarization reaches a detectable level of 1μrad. [1, p. 207]

2.2 Origin of decoherence

Spin decoherence in a particle bunch is caused by the difference in the spin precession angular velocities, which, in turn, is due to the difference in the particles' orbit lengths and momentum values. This can be seen from the following considerations.

When a particle with spin enters a magnetic field area, the spin vector starts turning about the magnetic field vector with an angular velocity defined by the T-BMT equation (**??**):

$$\boldsymbol{\Omega}_{MDM} = \frac{q}{m} G\boldsymbol{B}.$$

Upon exiting the field area, the spin has turned by an angle

$$\theta = \Delta t \cdot \Omega_{MDM} = \frac{L}{v} \cdot \frac{q}{m} GB \cdot \frac{\gamma_0}{\gamma_0} = \frac{L\gamma_0 GB}{B\rho} = \frac{L}{\rho}\gamma_0 \cdot G,$$

where L is the path length inside the B-field, and $B\rho = p/q$ is the magnetic rigidity.

In the simple model considered so far, the influence of the orbital dynamics upon the spin dynamics is expressed by the $\gamma_0 L/\rho$ (effective gamma) term. In the case of the reference particle, $\gamma_0 L/\rho = \gamma_0$, while for a particle involved in betatron motion, the effective gamma is different from γ_0. In the following sections we will specify the connection between the spin and orbital dynamics of a particle further in a more general fashion.

2.2.1 Equilibrium momentum shift

The longitudinal dynamics of a charged particle on the reference orbit in a storage ring is described by the system of equations:

$$\begin{cases} \frac{\mathrm{d}\varphi}{\mathrm{d}t} & = -\omega_{RF}\eta\delta, \\ \frac{\mathrm{d}\delta}{\mathrm{d}t} & = \frac{qV_{RF}\omega_{RF}}{2\pi h\beta^2 E}\sin\varphi. \end{cases}$$

In the equations above: φ is the phase deviation from the reference $\varphi_0 = 0$; $\delta = \frac{\Delta p}{p_0}$ is the relative momentum deviation from the momentum p_0 of the reference particle; V_{RF}, ω_{RF} are the voltage and oscilation frequency of the RF field; $\eta = \alpha_0 - \gamma^{-2}$ is the slip factor, with α_0 being the compaction factor defined by ${}^{\Delta L}/_{L} = \alpha_0\delta$, and L being the orbit length; h is the harmonic number; E is the total energy of the accelerated particle. $\omega_{RF} = 2\pi h f_{rev}$, where $f_{rev} = T_{rev}^{-1}$ is the beam revolution frequency.

The solutions of this system form a family of ellipses in the (φ, δ) space, centered at $(0, 0)$. However, if we consider a particle involved in betatron oscillations, and use a higher-order Taylor expansion of the compaction factor $\alpha = \alpha_0 + \alpha_1\delta$, the first equation of the system transforms into: [3, p. 2579]

$$\frac{\mathrm{d}\varphi}{\mathrm{d}t} = -\omega_{RF}\left[\left(\frac{\Delta L}{L}\right)_\beta + \left(\alpha_0 + \gamma^{-2}\right)\delta + \left(\alpha_1 - \alpha_0\gamma^{-2} + \gamma^{-4}\right)\delta^2\right],$$

where $\left(\frac{\Delta L}{L}\right)_\beta = \frac{\pi}{2L}\left[\varepsilon_x Q_x + \varepsilon_y Q_y\right]$, is the betatron motion-related orbit lengthening; ε_x and ε_y are the horizontal and vertical beam emittances, and Q_x and Q_y are the horizontal and vertical tunes. [3, p. 2580]

The solutions of the modified system are no longer centered at the same point. Orbit-lengthening and momentum deviation cause an equilibrium-level momentum momentum shift [3, p. 2581]

$$\Delta\delta_{eq} = \frac{\gamma_0^2}{\gamma_0^2\alpha_0 - 1}\left[\frac{\delta_m^2}{2}\left(\alpha_1 - \alpha_0\gamma^{-2} + \gamma_0^{-4}\right) + \left(\frac{\Delta L}{L}\right)_\beta\right], \tag{1}$$

where δ_m is the amplitude of synchrotron oscillations.

2.2.2 Effective Lorentz factor

The equilibrium energy associated with the momentum shift (1), termed the *effective Lorentz factor*, is [4]

$$\gamma_{eff} = \gamma_0 + \beta_0^2\gamma_0 \cdot \Delta\delta_{eq}, \tag{2}$$

where γ_0, β_0 are the reference particle's Lorentz factor and normalized speed. Equations (1) and (2) define the link between the particle spin and orbital dynamics.

2.3 Sextupoles for the reduction of decoherence

To minimize the spin decoherence dur to betatron motion and momentum deviation, sextupoles (or octupoles) may be used [1, p. 212]

A sextupole of strength

$$S_{sext} = \frac{1}{B\rho}\frac{\partial^2 B_y}{\partial x^2},$$

where $B\rho$ is the magnetic rigidity, affects the first-order compaction factor as [3, p. 2581]

$$\Delta\alpha_{1,sext} = -\frac{S_{sext}D_0^3}{L}, \tag{3}$$

and simultaneously the orbit length as

$$\left(\frac{\Delta L}{L}\right)_{sext} = \mp\frac{S_{sext}D_0\beta_{x,y}W_{x,y}}{L}, \tag{4}$$

where $D(s,\delta) = D_0(s) + D_1(s)\delta$ is the dispersion.

In the following sections, we will call the decoherence accociated with horizontal/vertical betatron, and synchrotron oscillations, respectively X-/Y-, and D-decoherence.

It can be observed from eqs equations (3, 4), that three sextupole families are required for the reduction of decoherence, placed in the maxima of: β_x, $beta_y$ for the reduction of X-,Y-decoherence, and D_0 for D-decoherence.

2.3.1 Simulation

In order to check the effectiveness of the sextupole method for the suppression of decoherence, a simulation was carried out using the COSY INFINITY code.

We took a perfectly aligned FS lattice, with three families of sextupoles (SX, SY, SD) placed as was explained at the end of section 2.3. Then we varied the strengths of each sextupole family (GSX, GSY, GSD) individually, and computed the spin tunes of particles offset at injection from the reference particle in: *a*) the x-coordinate for the SX-family, *b*) y-coordinate for the SY-family, and *c*) $d = \Delta K/K_0$ for the SD-family.

The spin tune depends parabolically for each direction of offset:

$$\mu(x,y,d) = \mu_0 + \mu_{xx}x^2 + \mu_{yy}y^2 + \mu_{dd}d^2 + O(x^3) + O(y^3) + O(d^3).$$

The search for the optimal sextupole strengths was done in two iterations:

1. first, we manually varied the strengths in a wide range, and observed the flattening of the spin tune curve;

2. when the global minima were found approximately, we continued the optimization automatically (for each family independently), using the second-order Taylor expansion coefficient before the corresponding coordinate.

The simulation results at 300 MeV (30 MeV above the FS energy) are presented in Figure 1. After the optimization of the sextupole strengths, spin tune shows almost no dependence on the variable offsets.[1]

3 Fake signal simulation

Systematic errors due to imperfections in the physical lattice, including optical element misalignments, are causative to a fake EDM signal. [1, p. 230] Rotational misalignments are particularly problematic, since they induce the horizontal magnetic error field components B_x and B_z both of which rotate spin in the vertical plane, thus causing a fake EDM signal.

Analytical estimates of the MDM precession frequency about the radial axis were made by Senichev. [4] From the T-BMT equation, and the expression for the Lorentz force, the MDM precession rate about the radial axis is

$$\sigma\left[\Omega_x^{MDM}\right] = \frac{q}{m\gamma}\frac{G+1}{\gamma}\frac{\sigma\left[B_x\right]}{\sqrt{n}}, \tag{5}$$

where n is the number of tilted spin rotators, and $\sigma\left[B_x\right] = B_y\sigma\left[\delta h\right]/L$, $\sigma\left[\delta h\right]$ being the alignment error standard deviation. At alignment error $\sigma\left[\delta h\right] = 100\mu$m, and deflector length $L = 1$m, $\sigma\left[\Omega_x^{MDM}\right] \approx 100$ rad/sec. [4]

We studied spin dynamics in the FS and QFS lattices in the presence of rotational magnet misalignments using the COSY INFINITY code. Our simulations appear to confirm the above analysis.

3.1 Error field implementation

In implementing field imperfections we followed the recommendations given in [1, p. 235]. A small perturbation of the magnetic field acts with a first-order perturbation correction as a small proportional rotation on the spin vector. Therefore, we implemented rotational magnet misalignments as an augmentation of the rotated elements with small, normally-distributed spin kicks.

According to eq (**??**), the MDM precession frequency change associated with an introduced error field $(B_x, 0, B_z)$ is

$$\Delta\Omega_{MDM} = \frac{q}{m}(B_x, 0, B_z),$$

so the spin kick angle is

$$\Theta_{kick} = t_0\Delta\Omega_{MDM},$$

where $t_0 = L/v_0$ is the time-of-flight of the reference particle through the element.

[1] We were unable to suppress all three types simultaneously in this lattice. Specifically, when the SD-type sextupoles are turned on, the D-decoherence is suppressed as before, but the X- and Y-types degrade even further.

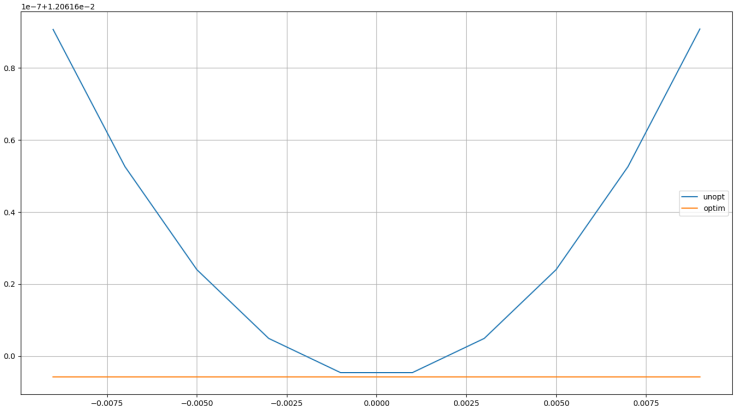

(a) GSX optimized for the X bunch

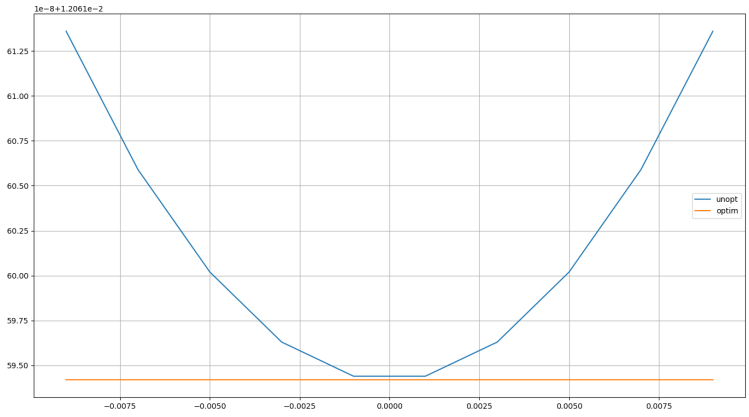

(b) GSY optimized for the Y bunch

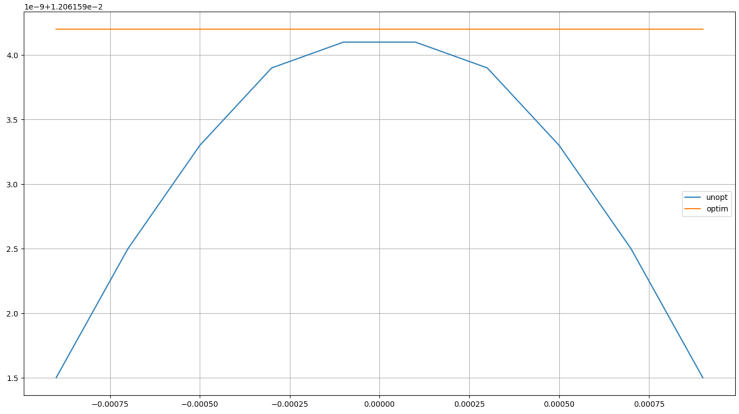

(c) GSD optimized for the D bunch

Figure 1: Spin tunes of offset particles vs the offsets, at 300 MeV, with/out the corresponding sextupole.

3.2 Simulation

We randomly assigned tilt angles Θ_{tilt} to E+B elements in the FS lattice. The experiment was performed 11 times; each time the angles were selected from a normal distribution $N(\mu_0 \cdot (i-5), \sigma_0)$, where $\mu_0 = 10 \cdot \sigma_0 = 10^{-4}$ rad, $i \in \{0, \ldots, 10\}$. After the construction of the 3rd order transfer map for the imperfect lattice, the spin tune and spin precession axis (SPA) Taylor expansions were computed. We then took the zero-order terms of the maps, representing the spin tune and SPA of the reference particle. The results are presented in Figure 2. In Figure 3 are shown the results when three pairs of E+B elements are rotated by opposite angles, and one element is rotated by an angle $\mu_i = (i-5) \cdot 10^{-6}$ rad, $i \in \{0, \ldots, 10\}$. The simulations were done at 270.0092 MeV.[2]

References

[1] Eremey Valetov. FIELD MODELING, SYMPLECTIC TRACKING, AND SPIN DECOHERENCE FOR EDM AND MUON G-2 LATTICES. Michigan State University. Michigan, USA;. Avail-

[2] At this energy the spin precession axis and spin tune are undefined in the beamline coordinate system used by COSY INFINITY in the perfect lattice. This corresponds to the situation when spin does not precess in any plane (horizontal or vertical), which is the FS condition in a perfect lattice.

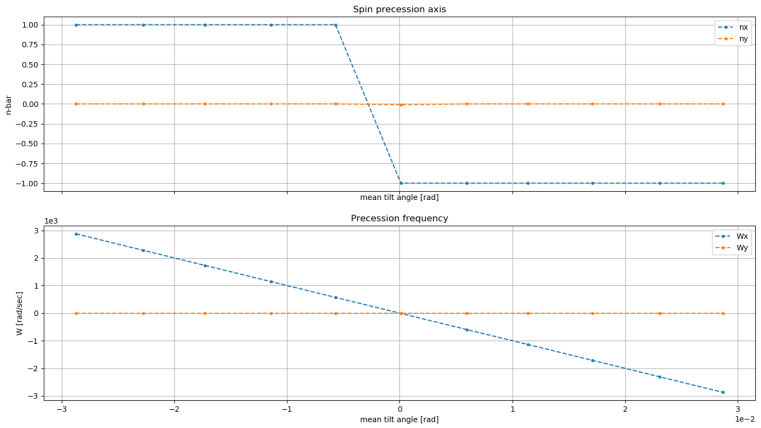

Figure 2: Spin precession axis and precession frequencies for the imperfect FS lattice, under the rotation of E+B elements.

able from: http://collaborations.fz-juelich.de/ikp/jedi/public_files/theses/valetovphd.pdf.

[2] D Anastassopoulos, V Anastassopoulos, D Babusci. AGS Proposal: Search for a permanent electric dipole moment of the deuteron nucleus at the 10 29 e cm level. BNL; 2008. Available from: https://www.bnl.gov/edm/files/pdf/deuteron_proposal_080423_final.pdf.

[3] Senichev Y, Zyuzin D. SPIN TUNE DECOHERENCE EFFECTS IN ELECTRO- AND MAGNETOSTATIC STRUCTURES. In: Beam Dynamics and Electromagnetic Fields. vol. 5. Shanghai, China: JACoW; 2013. p. 2579–2581. OCLC: 868251790. Available from: https://accelconf.web.cern.ch/accelconf/IPAC2013/papers/wepea036.pdf.

[4] Yury Senichev. Frequency domain method of the search for the deuteron electric dipole moment in a storage ring with imperfections;. Available from: https://mail-attachment.googleusercontent.com/attachment/u/0/?ui=2&ik=7fc6107b60&view=att&th=15d604450498d398&attid=0.1&disp=safe&zw&saddbat=ANGjdJ8kSdMTQUkpPWe6xjODjjLdP-xU7StU6dUW7RLGZ3yMcR06cF3dymVY89FbIIJLxgcHSSJLgWX4iK_XfdvgOGSJyuav2kRjMKdvRL4Hb-NZqtKdC2SQlsMFlwwJlI_vSCXwew-6R9HRaBMjVsRreHlULw3i9QtP0lzMGXHwGH4Mf0JkdGhwYfxhpI6WStzajdQibfA0oFRyEl861YacE3H47HPH7gIk-qt2wNCgq-Vc6F97QozjqLYPeRq0SfxkALLCGJlhF1kJP3p9eL9fKbOqTl5JW2gZl-kEJvh5GWnJ-EhaDPcMW7JZNAi1hUqNUJ25jZTWB3PTdsaXUpkD-tMav1RH0Dj5hBK9zJhonZmtxX4R6vZ1SqEv-myKWFeS7NBZ1gY5

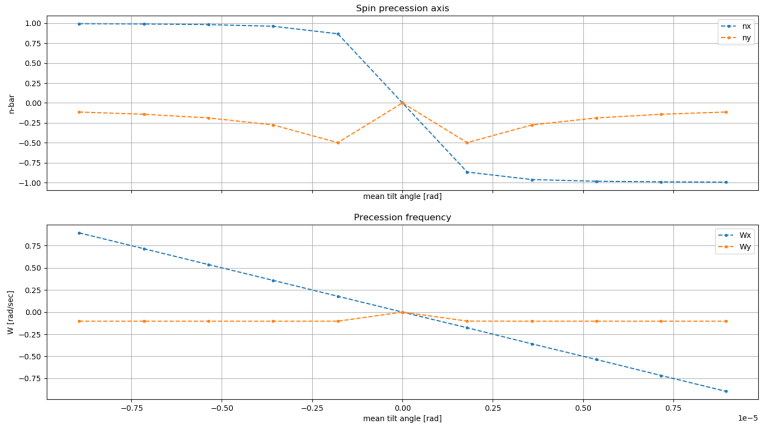

Figure 3: Three pairs of oppositely rotated E+B elements, plus an uncompensated element.